Journal of Engineering Mathematics 19 (1985) 157–172.

Prediction of leading-edge vortex behaviour to supplement the suction analogy

N. RILEY * and J.H.B. SMITH **

* *School of Mathematics and Physics, University of East Anglia, Norwich, UK;* ** *Aerodynamics Department, Royal Aircraft Establishment, Farnborough, Hants., UK*

(Received March 12, 1985)

Summary

An analytical treatment is presented which permits the prediction of the strength and path of leading-edge vortices on thin wings of delta-like planform from a knowledge of the behaviour of the linearized approximation to the attached flow past the wing. This supplements the leading-edge suction analogy, which predicts the forces and moments acting on the wing from the same input. The fundamental assumption is that the vortex lies close to the leading edge. It is represented by a single line-vortex and the presentation is confined to low-speed flow and plane wings. The treatment is independent of the way the basic attached flow is calculated. Results are shown for two simple planforms, using inputs from three-dimensional lifting-surface theory and from slender-body theory.

1. Introduction

The leading-edge suction analogy of Polhamus [1], as developed in a series of papers from the Langley Research Center of the NASA, has proved a useful tool for predicting the forces and moments on sharp-edged wings with leading-edge vortices. However, it does not provide any information about the behaviour of the vortices themselves. Methods capable of predicting the strength and position of the vortices are either more complex and expensive to use or fall back on the approximations of slender-body theory. The present paper describes a method for calculating the strength and position of the vortices within the framework of lifting-surface theory and the suction analogy, with little additional computation. In its present form, the method is limited to plane wings at low speeds, and to flows involving the formation of a single vortex from each leading edge, but extensions are easily envisaged.

The method rests on two assumptions. Fundamentally, we suppose that the leading-edge vortex lies in the immediate neighbourhood of the leading edge, as it does at small angles of incidence. The second assumption is that the vortex can be represented by the combination of a line-vortex and a cut joining the line-vortex to the leading edge, as in the treatment of Brown and Michael [2]. There is numerical evidence [3,4] that this is a good approximation to the vortex-sheet model at small angles of incidence. The first assumption enables the problem to be expressed in a two-dimensional form; the second assumption makes the solution of that problem very simple. The analytic form of the solution found resembles that which arises from the further assumptions of slender-body theory, but the numerical magnitudes are significantly different.

As examples, two planforms with semi-apex angles of about 27° are considered, one a delta of aspect ratio 2, and the other a "mild gothic", with a streamwise tip and a curved leading edge. Numerical results are presented for the position and strength of the vortex by the present treatment and by slender-body theory.

2. Analysis

We consider the flow of an essentially incompressible uniform inviscid stream of speed U past a plane wing at a small angle of incidence α. The leading edges of the wing are swept back through a local angle Λ, and are sharp enough for the flow to separate along them. The thickness of the wing is ignored. We use a Cartesian coordinate system (X, Y, z) to describe the global flow, with origin at the wing apex, OX along the wing centre-line, OY to startboard and Oz upwards, as in fig. 1. To describe the flow near the starboard leading edge, we introduce a local orthogonal coordinate system. The leading edge itself is a coordinate line, and x is the distance measured along it in the downstream sense; y is the distance along the outward normal to the leading edge in the plane of the wing, and z is the distance normal to the wing plane. The element of length in the x-direction is $h(x, y)\mathrm{d}x$, where $h(x, 0) = 1$; the elements of length in the other directions are $\mathrm{d}y$ and $\mathrm{d}z$. Then the velocity potential, Φ, of the three-dimensional flow satisfies the continuity equation

$$\frac{\partial}{\partial x}\left(\frac{1}{h}\frac{\partial \Phi}{\partial x}\right)+\frac{\partial}{\partial y}\left(h\frac{\partial \Phi}{\partial y}\right)+\frac{\partial}{\partial z}\left(h\frac{\partial \Phi}{\partial z}\right)=0. \tag{1}$$

Φ must also satisfy the appropriate boundary conditions: its normal derivative vanishes

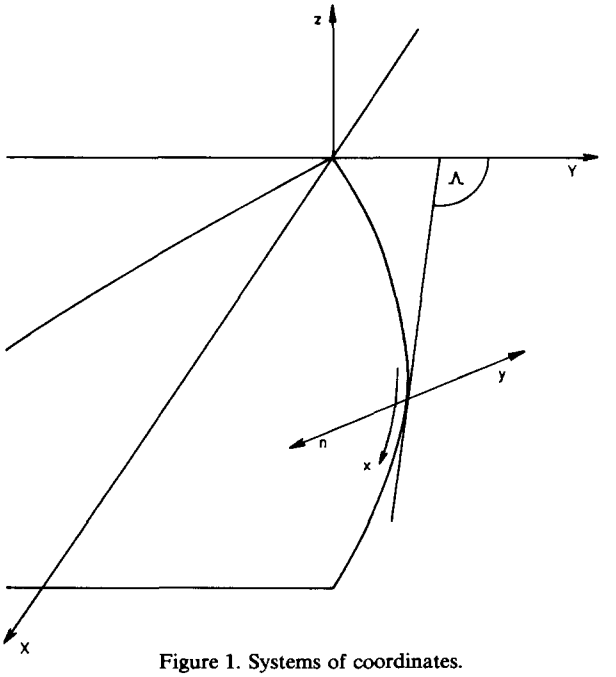

Figure 1. Systems of coordinates.

on the wing and it behaves like a uniform stream at large distances. Since the angle of incidence is small, we can expand Φ in powers of α,

$$\Phi = \Phi_0 + \alpha\Phi_1 + \cdots, \tag{2}$$

where Φ_0 is the potential of the uniform stream and $\alpha\Phi_1$ is the first-order approximation to the disturbance potential due to the wing at incidence.

The defect of this conventional attached-flow solution is that it does not satisfy a Kutta condition at the sharp leading edge. We accommodate this non-uniformity of the solution at the leading edge by introducing a representation of the circulation which is shed from the edge. For small angles of incidence, the circulation will be confined to the neighbourhood of the edge itself, and it emerges that the flow there may be treated in the slender-body approximation, so that the expansion technique of Clark, Smith and Thompson [5] may be employed. To establish this formally, we suppose that $\delta(\alpha)$ is the length-scale of the vortex configuration at the leading edge, with

$$\delta(\alpha) \to 0 \quad \text{as } \alpha \to 0. \tag{3}$$

δ is then the scale of the "inner" region, in which we introduce scaled variables distinguished by a tilde,

$$y = \delta\tilde{y}, \qquad z = \delta\tilde{z}, \qquad \Phi = M(x)U + \delta\tilde{\phi}. \tag{4}$$

Here

$$M'(x) = \sin \Lambda(x) \tag{5}$$

since

$$h(x, y) = h(x, 0) + O(y) = 1 + O(\delta).$$

Introducing (4) in (1), we see that, to leading order in δ, $\tilde{\phi}$ satisfies the two-dimensional Laplace equation

$$\frac{\partial^2\tilde{\phi}}{\partial\tilde{y}^2} + \frac{\partial^2\tilde{\phi}}{\partial\tilde{z}^2} = 0. \tag{6}$$

The derivation requires that $\delta\Lambda'(x) \ll 1$, so that the treatment may fail for leading edges with kinks.

Any solution of (6) can be expressed as the real part of a complex analytic function of $\tilde{Z} = \tilde{y} + \mathrm{i}\tilde{z}$. In particular, we may write the inner complex potential in the form

$$\tilde{W} = UB(x, \delta)\tilde{Z} - \mathrm{i}U\delta_1 A(x)\tilde{Z}^{1/2} + f(\tilde{Z}). \tag{7}$$

In (7) the leading term corresponds to the component of the onset flow in the plane of the wing and normal to the leading edge, with B real. On the scale of the inner region, the wing is a semi-infinite plate, occupying the negative real axis of the $\tilde{Z}$-plane. The second term in (7) represents the flow around this plate. δ_1, which depends on δ, is a real scale factor to be determined later; and, with A real, the negative real axis is a streamline. The

singular behaviour of the second term in (7) is related to the leading-edge suction force perpendicular to the edge in the plane of the wing; $A(x)$ will be determined from the strength of this suction force in the outer solution. The final term in (7) is the contribution from the model of the vortex flow. It must be chosen so as to cancel the singular behaviour of the second term at the leading edge, to preserve the boundary condition on the semi-infinite plate, and to decay as $\tilde{Z} \to \infty$.

In accordance with the standard procedure for matching asymptotic expansions [6], we form the outer expansion of (7), expressing it in the outer, physical, variables,

$$W = UB_0(x)Z - \mathrm{i}U\delta_1\delta^{1/2}A(x)Z^{1/2} + O(\delta),$$

where $B_0(x) = B(x, 0)$ and $Z = y + \mathrm{i}z = r\,\mathrm{e}^{\mathrm{i}\theta}$. Taking the real part, we have

$$\phi = UB_0(x)y + U\delta_1\delta^{1/2}A(x)r^{1/2}\sin(\theta/2) + O(\delta). \tag{8}$$

This is to be compared with the inner expansion of the outer solution, which has so far only been expressed in the form of (2). We see at once from the terms of zero order in the small parameter α that

$$B_0(x) = -\cos\Lambda(x). \tag{9}$$

To obtain a term of order α from (8) we must choose $\delta_1\delta^{1/2}$ to be of order α, so that, with the constant of proportionality absorbed in $A(x)$,

$$\delta_1 = \alpha\delta^{-1/2}(\alpha). \tag{10}$$

To determine $A(x)$, we suppose we have a solution for the attached flow past the wing, in the small disturbance approximation, say from lifting surface theory. This provides the loading coefficient

$$\Delta C_p = C_{p_{\text{lower}}} - C_{p_{\text{upper}}}, \tag{11}$$

from which it is possible to obtain a measure of the strength of the leading-edge singularity at a point x,

$$G(x) = \lim_{n\to 0} n^{1/2}\Delta C_p(x, n), \tag{12}$$

where n $(= -y)$ is the distance inboard of the leading edge along the normal to it. Now, in the small disturbance approximation,

$$\Delta C_p = -\frac{2}{U}\frac{\partial\Delta\phi}{\partial X}.$$

From (8) and (10),

$$\Delta\phi = -2\alpha UA(x)n^{1/2}.$$

Hence

$$\frac{\partial \Delta\phi}{\partial X} = \frac{\partial \Delta\phi}{\partial x}\frac{\partial x}{\partial X} + \frac{\partial \Delta\phi}{\partial n}\frac{\partial n}{\partial X} = -2\alpha U\left(A'(x)\sin\Lambda\, n^{1/2} + \tfrac{1}{2}A(x)\cos\Lambda\, n^{-1/2}\right),$$

so that $A(x)$ is given by

$$G(x) = 2\alpha A(x)\cos\Lambda(x). \tag{13}$$

Note that A, like G, is a dimensional quantity.

We must now construct the last term in (7), choosing the simplest representation of the leading-edge vortex, the single line-vortex and cut, as used by Brown and Michael [2]. In order to simplify the treatment of the boundary condition on the semi-infinite plate, we use the mapping

$$\zeta = \tilde{Z}^{1/2}, \tag{14}$$

which unfolds the negative real axis on to the imaginary axis in the ζ-plane. With a line-vortex of strength $\tilde{\Gamma}$ at the point $\zeta = \zeta_V$, and its image in the imaginary axis, (7) becomes

$$\tilde{W} = UB(x,\delta)\zeta^2 - \mathrm{i}U\delta_1 A(x)\zeta + \frac{\tilde{\Gamma}}{2\pi\mathrm{i}}\ln\frac{\zeta-\zeta_V}{\zeta+\bar{\zeta}_V}. \tag{15}$$

$\tilde{\Gamma}$ and ζ_V are determined from the Kutta condition at the leading edge, and the condition that the total transverse force on the combination of the vortex and the cut joining it to the edge is zero. The Kutta condition of finite velocity at the origin of the $\tilde{Z}$-plane implies $\mathrm{d}\tilde{W}/\mathrm{d}\zeta = 0$ at $\zeta = 0$, so that

$$\tilde{\Gamma} = \frac{2\pi U\delta_1 A\zeta_V\bar{\zeta}_V}{\zeta_V + \bar{\zeta}_V}. \tag{16}$$

The force on the line vortex arises from its inclination to the local flow direction, the transverse force per unit length being given by $-\mathrm{i}\rho\tilde{\Gamma}$(velocity of fluid relative to vortex); this is equal to

$$-\mathrm{i}\rho\tilde{\Gamma}\left(v_1 + \mathrm{i}w_1 - \frac{\mathrm{d}}{\mathrm{d}x}(MU)\delta\frac{\mathrm{d}\tilde{Z}_V}{\mathrm{d}x}\right). \tag{17}$$

Here $v_1 + \mathrm{i}w_1$ is the velocity induced at the vortex in the plane normal to the leading edge, given by

$$v_1 - \mathrm{i}w_1 = \lim_{Z\to Z_V}\left(\frac{\mathrm{d}\tilde{W}}{\mathrm{d}\tilde{Z}} - \frac{\tilde{\Gamma}}{2\pi\mathrm{i}}\frac{1}{\tilde{Z}-\tilde{Z}_V}\right); \tag{18}$$

and the second term in (17) comes from the inclination of the line vortex to the velocity component along the leading edge given by the first term of (4). We have again replaced $h(x, y)$ by $h(x, 0) = 1$. The force on the cut arises from the pressure difference across it,

which is due to the growth in the strength of the vortex. The change in vortex strength implies a jump across the cut of $\mathrm{d}\tilde{\Gamma}/\mathrm{d}x$ in the component of velocity in the direction of x increasing, so that Bernoulli's theorem enables the jump in pressure across the cut to be obtained as

$$-\rho\frac{\mathrm{d}}{\mathrm{d}x}(MU)\frac{\mathrm{d}\tilde{\Gamma}}{\mathrm{d}x}.$$

The length of the cut is $\delta|\tilde{Z}_{\mathrm{V}}|$, so the force on it, per unit length of the vortex, is

$$\mathrm{i}\rho\frac{\mathrm{d}}{\mathrm{d}x}(MU)\frac{\mathrm{d}\tilde{\Gamma}}{\mathrm{d}x}\delta\tilde{Z}_{\mathrm{V}}.$$

Equating to zero the sum of this and expression (17) gives, using (5),

$$\tilde{\Gamma}(v_1+\mathrm{i}w_1)=\delta U\sin\Lambda\frac{\mathrm{d}}{\mathrm{d}x}(\tilde{\Gamma}\tilde{Z}_{\mathrm{V}}). \tag{19}$$

Introducing (15) into (18) and making use of (14) and (16) leads to

$$v_1-\mathrm{i}w_1=UB(x,\delta)-\tfrac{1}{4}\mathrm{i}U\delta_1A(x)\left(\frac{1}{\zeta_{\mathrm{V}}}+\frac{\zeta_{\mathrm{V}}-\tilde{\zeta}_{\mathrm{V}}}{(\zeta_{\mathrm{V}}+\bar{\tilde{\zeta}}_{\mathrm{V}})^2}\right). \tag{20}$$

To split (19) into its real and imaginary parts we introduce

$$\zeta_{\mathrm{V}}=\sigma+\mathrm{i}\tau. \tag{21}$$

Then, with v_1 and w_1 given by (20), and $\tilde{\Gamma}$ given by (16), the real and imaginary parts of (19) can be written as

$$\frac{A(x)(\sigma^2+\tau^2)}{\sigma}\left(B(x,\delta)-\frac{\delta_1A(x)\tau(\sigma^2-\tau^2)}{8\sigma^2(\sigma^2+\tau^2)}\right)=\delta\sin\Lambda(x)\frac{\mathrm{d}}{\mathrm{d}x}\left(A(x)\frac{\sigma^4-\tau^4}{\sigma}\right) \tag{22}$$

and

$$\tfrac{1}{8}\delta_1A^2(x)=\delta\sin\Lambda(x)\frac{\mathrm{d}}{\mathrm{d}x}(A(x)\tau(\sigma^2+\tau^2)). \tag{23}$$

Now, by virtue of the original scaling, neither σ nor τ will tend to infinity as α tends to zero. Hence the right-hand side of (22) will be of higher order than the left, and a balance between the two terms of lowest order can only be obtained if σ^2 is of the same order as δ_1. Writing

$$\sigma=\delta_1^{1/2}\sigma_0+\cdots,\qquad \tau=\tau_0+\cdots, \tag{24}$$

we see from (22) that

$$B_0(x) + \frac{A(x)\tau_0}{8\sigma_0^2} = 0. \tag{25}$$

With (24), the terms in (23) can only balance if δ_1 and δ are of the same order. Taking $\delta_1 = \delta$, so that, by (10),

$$\delta_1 = \delta = \alpha^{2/3}, \tag{26}$$

we find from (23) that

$$\tau_0^3 = \frac{1}{8A(x)} \int_0^x \frac{A^2(\xi)\mathrm{d}\xi}{\sin \Lambda(\xi)}, \tag{27}$$

where ξ is an integration variable corresponding to x, and x is measured from the point of origin of the vortex, e.g. the wing apex. It is perhaps worth pointing out, in relation to (27), that both τ_0 and A have the dimensions of (length)$^{1/2}$.

Since $A(x)$ and $B_0(x)$ are determined by (13) and (9) in terms of the outer solution for attached flow and the planform shape, (27) and (25) determine the functions $\tau_0(x)$ and $\sigma_0(x)$. In terms of these, the vortex positions can be expressed, to leading order, in the original outer variables by (4), (14), (24) and (26) as

$$y_V = -\alpha^{2/3}\tau_0^2, \qquad z_V = 2\alpha\sigma_0\tau_0. \tag{28}$$

The strength, Γ, of the vortex in the outer variables is related to $\tilde{\Gamma}$ in the same way as ϕ is related to $\tilde{\phi}$; so, by (4), $\Gamma = \delta\tilde{\Gamma}$. Then, using (21), (24) and (26) in (16), we find

$$\Gamma = \pi\alpha U A \tau_0^2/\sigma_0 \tag{29}$$

$$= 4\pi U z_V \cos \Lambda, \tag{30}$$

by (25) and (28).

The form of the variation of the vortex position and circulation with the angle of incidence is the same as that which arises from the use of slender-body theory [5] under the same assumption of small α. The difference arises from the determination of $A(x)$, which can be written in closed form in the slender-body approximation.

It is worth pointing out that, although in this very simple treatment the properties of the vortex are determined by the behaviour of the attached flow, they are not determined by its local behaviour. The integration process involved in (27) represents, in the most elementary way, the principle of the convection of circulation. This is in contrast to the determination of non-linear lift in the leading-edge suction analogy, by which the local lift is related to the local behaviour of the attached flow.

Before going on to illustrate this analytical solution with numerical examples, we consider briefly how the expansion would be extended to higher order in the angle of incidence. In order to find the form of the next term in the outer expansion (2), we consider the outer expansion of the inner solution (7). The first and second terms in the

expansion (7) match with those in (2). The outer dependent variable corresponding to the third term in (7) is

$$\delta f(\tilde{Z}) = \frac{\delta\tilde{\Gamma}}{2\pi i}\ln\frac{\zeta-\zeta_V}{\zeta+\bar{\zeta}_V} = -\frac{\Gamma}{2\pi i}\frac{\zeta_V+\bar{\zeta}_V}{\zeta} + O(\zeta^{-2}).$$

The outer independent variable is $Z = \delta\tilde{Z} = r\,e^{i\theta}$, so

$$\mathrm{Re}\{\delta f(\tilde{Z})\} = \alpha^{5/3}UA\tau_0^2 r^{-1/2}\sin\theta/2 + \cdots. \tag{31}$$

Equation (31) shows that, to effect a match with the inner solution, the expansion (2) must contain a term of order $\alpha^{5/3}$. If the coefficient of this term is denoted by ϕ_2, then ϕ_2 is required to be a solution of Laplace's equation (1), to vanish at infinity, to have zero normal derivative on the wing surface, to behave asymptotically like (31) at each leading edge, and to satisfy a Kutta condition at the trailing edge. Calculating ϕ_2 would clearly be a formidable problem, which would have to be tackled before further terms in (7) could be constructed.

3. Examples

As pointed out earlier, the present assumptions break down at a discontinuity in the slope of the planform's leading edge. We therefore consider only planforms for which each leading edge forms a smooth curve. Since we are interested in vortex flows we also assume that the planform has a pointed apex from which the vortices originate. Planforms of this kind which are of practical interest have their leading and trailing edges meeting at an angular tip. Some degree of unreality must be expected in the solution at such a tip, since in the neighbourhood of the tip there is no length scale on which the wing resembles a semi-infinite plate. It turns out that different forms of unreality arise for delta wings and for wings with streamwise tips, so we consider one example of each kind.

It is convenient to describe the planform by writing its local semi-span, s, as a function of the lengthwise distance, X, from the apex of the wing. The starboard leading edge is then given by $Y = s(X)$. Then

$$\cos\Lambda = s'(1+s'^2)^{-1/2}, \qquad \sin\Lambda = (1+s'^2)^{-1/2},$$

and the element of length along the leading edge is

$$\mathrm{d}x = (1+s'^2)^{1/2}\mathrm{d}X.$$

Then (27) becomes

$$\tau_0^3 = \frac{1}{8A(X)}\int_0^X A^2(t)(1+s'^2)\mathrm{d}t, \tag{32}$$

where A is now regarded as a function of X, and t is a variable of integration.

The starboard halves of the two planforms are shown in Fig. 2. The first is a delta wing of aspect ratio 2, for which Λ is between 63° and 64°. The second is a "mild gothic" wing

Figure 2. Planforms considered.

of aspect ratio 1.385. The planforms of this family have streamwise tips, but are closer to the delta form than is the more familiar parabolic gothic. The shape is specified by the local semi-span,

$$s(X) = 0.25s(c)\left(\frac{5X}{c} - \left(\frac{X}{c}\right)^5\right), \tag{33}$$

with the trailing edge at $X = c$. For an aspect ratio of 1.385, we have

$$s(c) = 0.404c. \tag{34}$$

As can be seen, the forward parts of the wings are very similar.

The lifting-surface theory program used to calculate G, and so determine A, is an unpublished program written by C.C. Lytton (formerly C.C.L. Sells) at RAE, and briefly described in [7]. In Fig. 3 the variation of A with the lengthwise coordinate X for the two planforms is shown by the solid lines.

The two curves run together near the apex, reflecting the similar planform shapes there. The nature of the behaviour at the apex could be elucidated using the work of Medan [8],

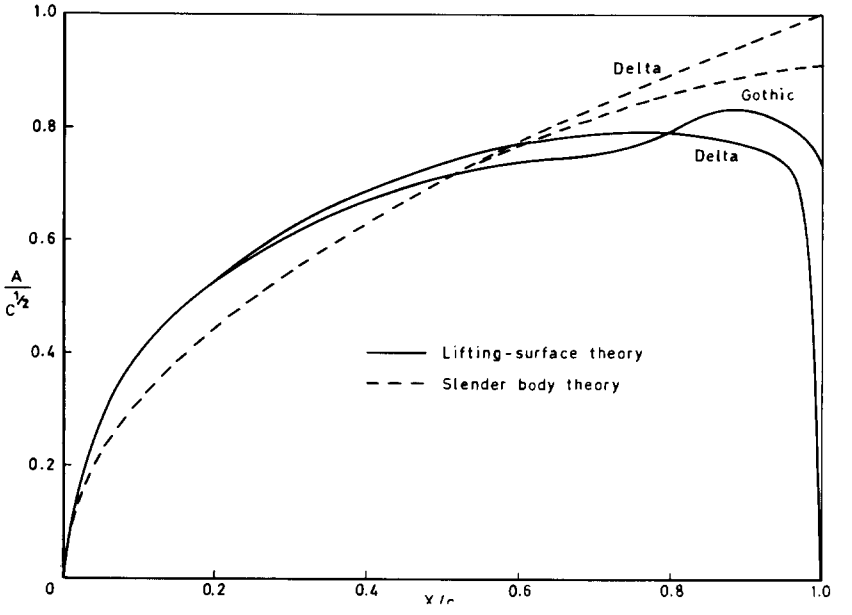

Figure 3. Strength of leading-edge singularity in attached flow.

but this is not necessary for the present purpose. For the delta wing, Λ is constant, so that A behaves like G, the strength of the singularity in the loading at the leading edge. This falls towards the rear of the wing, because of the upstream influence of the trailing edge. Very close to the tip, this fall becomes precipitous, and the behaviour is explained in the Appendix, with the help of Medan's results [8]. For the mild gothic wing, cos Λ also falls to zero at the tip, and it emerges that A remains finite and non-zero there. On the forward part of the wing, where Λ is very similar for the two planforms, A behaves like G, and is lower for the gothic because its span is smaller. Further back, the fall in cos Λ on the gothic leads to values of A which exceed those for the delta.

Values of A calculated by slender-body theory for the same planforms are shown by broken lines in Fig. 3. The two curves now lie together for more of the length, because the solution upstream is unaffected by the smaller overall span of the gothic wing. For the delta wing, the linear growth of A is maintained to the tip, unaffected by the existence of the trailing edge. Over the forward part of the wings, slender-body theory underestimates the value of A because it ignores the upwash induced by the bound vorticity further aft. Despite these differences, slender-body theory provides a good overall estimate of A for the mild gothic planform.

For this mild gothic planform, the results of using the lifting-surface theory values of A to determine successively τ_0 by (32), σ_0 by (9) and (25), z_V by (28) and Γ by (30) are shown by the curves labelled "outer" in figs. 4 and 5. The indefinite increase of z_V towards the trailing edge and the vanishing of Γ there both arise because σ_0 and σ increase indefinitely. This rapid rate of change of σ means that (25) is not a valid approximation to (22) near the trailing edge, because the term on the right is large. This difficulty is resolved in the Appendix, by the introduction of a further inner expansion, this time centred on the trailing edge. By combining this inner expansion with the solution already derived and valid away from the trailing edge, which is labelled "outer" in Figs. 4

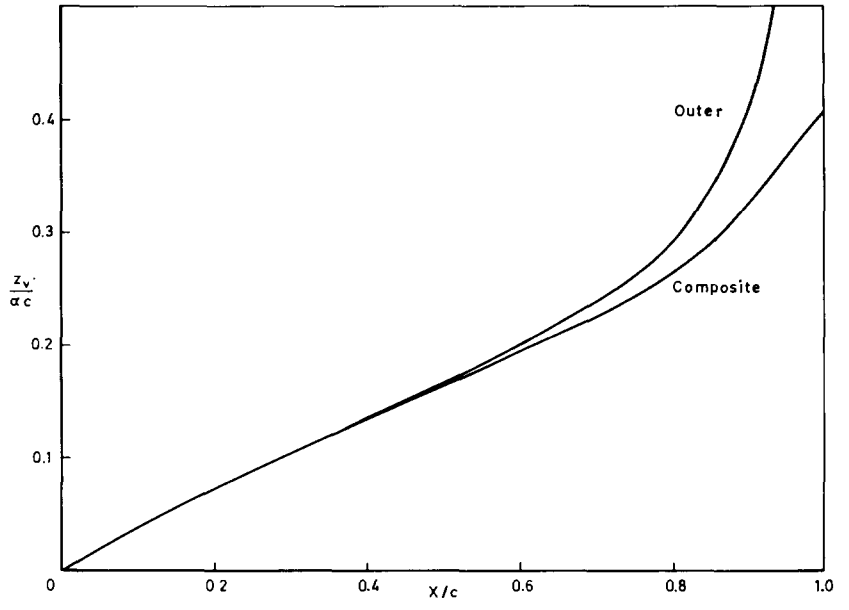

Figure 4. Mild gothic planform: height of vortex above wing.

and 5, into a composite expansion valid along the whole leading edge, the more realistic solutions labelled "composite" in Figs. 4 and 5 are obtained. An unfortunate complication is that the composite solution involves more than one power of the angle of incidence. Thus, although the outer solution represented in Figs. 4 and 5 is independent of α, the composite solution is only exact for a particular value of α, chosen to be 10°. It is approximately correct for other values, and the exact solution for other values can easily be obtained from the equations in the Appendix. The inboard displacement, y_V, of the

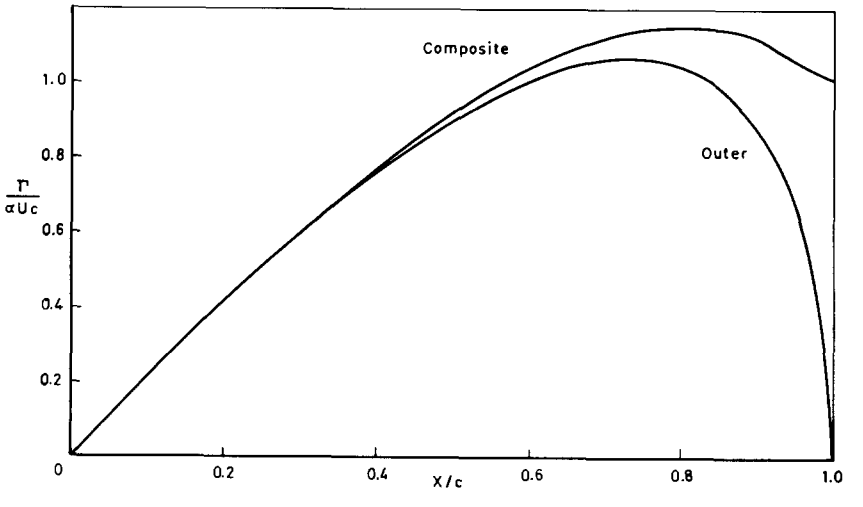

Figure 5. Mild gothic planform: circulation of vortex.

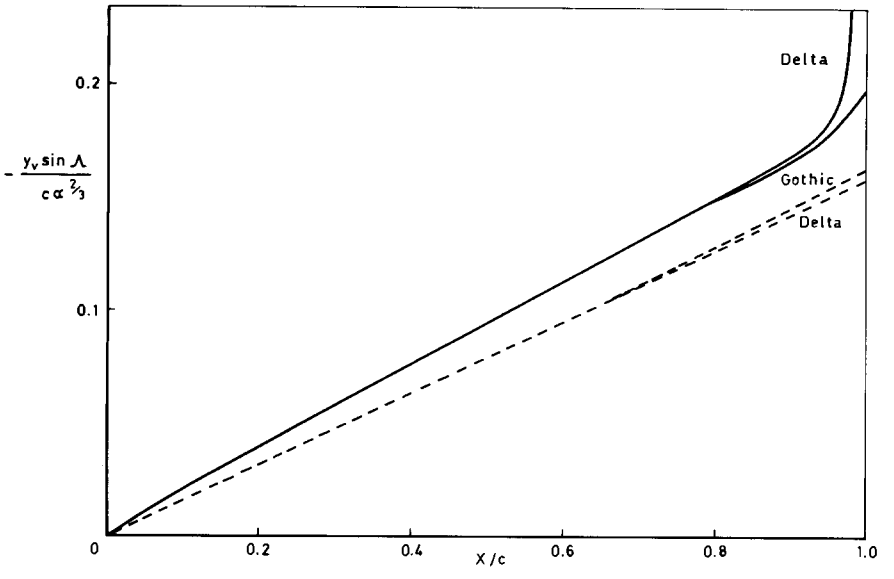

Figure 6. Inboard displacement of vortex from leading edge; symbols as in Fig. 3.

vortex is not affected by this modification of the solution near the trailing edge, and no modification is required for the delta wing. The results for vortex height and strength on the mild gothic wing discussed below are all for composite solutions at $\alpha = 10°$, whether they derive from lifting-surface theory or slender-body theory.

Figures 6 to 8 show the position and strength of the leading-edge vortex for each of the four determinations of A represented in Fig. 3, i.e. for the two planforms and the two

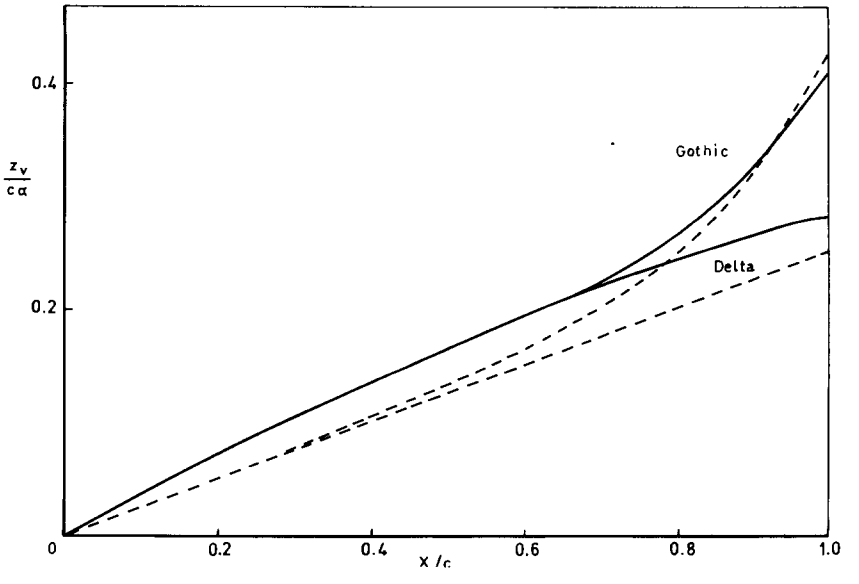

Figure 7. Height of vortex above wing; symbols as in Fig. 3.

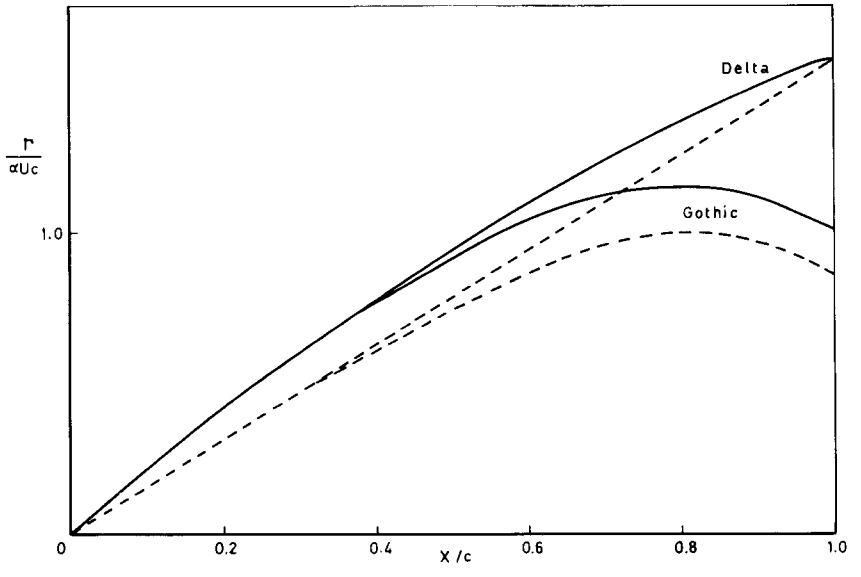

Figure 8. Circulation of vortex; symbols as in Fig. 3.

theories. To obtain the spanwise displacement of the vortex inboard of the leading edge, $(-y_V)$ has been multiplied by sin Λ, and this is shown in Fig. 6. For the case of the delta wing with A found from lifting-surface theory, the inboard displacement diverges to infinity in the immediate neighbourhood of the trailing edge as a consequence of the sudden fall of A to zero. This unreal behaviour is interpreted as meaning that the inboard displacement of the real vortex no longer scales with $\alpha^{2/3}$ as the trailing edge is approached. Observation of real flows shows vortices lying almost streamwise, in plan view, where they cross the trailing edge.

Apart from this local divergence, the inboard displacement of the vortex is scarcely affected by the presence or absence of the streamwise tip. In contrast, Figs. 7 and 8 show that both the height and circulation of the vortex are very different over the rear of the two planforms. (Note that the results for the gothic wing are based on the composite expansion.) On the wing with the streamwise tip the vortex is weaker and lies further above the wing than it does on the wing with the straight leading edge. Similar behaviour was found by Clark [9], using a vortex sheet model. He was able to identify the circulation of the opposite hand which was shed from the leading edge to produce the reduction in total circulation. Over the forward part of the wings, where the planforms are almost the same, the differences in vortex behaviour are small.

The differences between the predictions of the different theories tend to be greatest over the forward part of the wings. This seems to arise because slender-body theory underestimates the strength of the edge singularity forward and overestimates it aft, and the effects of these discrepancies tend to balance over the rear part. Lifting-surface theory puts the vortex further inboard than slender-body theory, bringing it closer to the observed position. However, the change is small compared with the difference between the predictions of the single line-vortex model and the vortex-sheet model. Over the forward parts of the wings, slender-body theory considerably underestimates both the height and strength of the vortex, but this difference becomes smaller over the rear. The differences

are smaller for the mild gothic wing than for the delta wing, but it is not clear from the present limited comparison how far this is an effect of aspect ratio and how far it depends on planform type.

4. Conclusions

An analysis has been presented which leads to a simple description of the behaviour of the leading-edge vortices on thin, sharp-edged wings at small angles of incidence. The description relies on the same input from lifting-surface theory as the leading-edge suction analogy used to estimate the nonlinear forces and moments.

A comparison with the use of slender-body theory shows differences which are not large, but might be significant. A comparison between two planforms of similar apex angles shows differences arising from the presence of a streamwise tip which are similar to those found earlier with a more elaborate, vortex-sheet, model in the framework of slender-body theory.

Appendix: Tip behaviour

Suppose that, as the tip is approached along the leading edge, the behaviour of the edge singularity and the sweep is described by

$$G(x) \sim k_1(x_t - x)^m \quad \text{and} \quad \cos \Lambda(x) \sim k_2(x_t - x)^n,$$

where suffix t denotes the value at the tip. Then the corresponding exponents in the quantities of interest are determined in sequence as follows:

$$\begin{aligned} &B(x): n, && \text{by (9)}; && A(x): m-n, && \text{by (13)}; \\ &\tau_0: \tfrac{1}{3}(n-m), && \text{by (27)}; && \sigma_0: \tfrac{1}{6}(2m-5n), && \text{by (25)}; \end{aligned} \tag{A.1}$$

$$y_V: \tfrac{2}{3}(n-m), \qquad z_V: -\tfrac{1}{2}n, \quad \text{by (28)};$$

$$\Gamma: \tfrac{1}{2}n, \quad \text{by (29)}.$$

For a delta wing, $n = 0$; and for a regular (locally parabolic) streamwise tip, $n = 1$. Values of m for a delta wing follow directly from the work of Medan [8]; for a streamwise tip we resort to a plausible extension of his treatment.

With polar coordinates r and θ centred on a corner of the planform he shows the asymptotic behaviour of the disturbance potential is

$$\phi \sim r^s f(\theta) \quad \text{for } r \text{ small.} \tag{A.2}$$

The exponent s depends on the angle at the corner: for the tip where a leading edge of local sweepback Λ_t meets an unswept trailing edge, a minor extrapolation of Medan's calculations yields the values given in Table 1. The exact values for $\Lambda_t = 0$ and 90° are $s = 1$ and 0.5. For the delta wing it is convenient to measure θ from the leading edge. The familiar square-root behaviour at the leading edge means that (A.2) can be rewritten

$$\phi \sim K r^s \theta^{1/2} \tag{A.3}$$

Table 1

Λ_t	10°	20°	30°	40°	50°	60°	70°	80°
s	0.952	0.893	0.829	0.762	0.699	0.641	0.589	0.542

for θ and r both small. Hence, to leading order,

$$\phi_X \sim \tfrac{1}{2} K r^{s-1} \theta^{-1/2} \cos \Lambda_t,$$

and so, by (12),

$$G = \lim_{\theta \to 0} (r\theta)^{1/2} \frac{4}{U} \phi_X \sim \frac{2K}{U} r^{s-1/2} \cos \Lambda_t. \tag{A.4}$$

For a wing with a curved streamwise tip we need a plausible generalization of (A.3). If the tip is defined by $\theta = g(r)$, with θ measured from the tangent to the leading edge at the tip, so that $g(0) = 0$, we propose the form

$$\phi \sim K r^{1/2} (\theta - g(r))^{1/2} \tag{A.5}$$

for θ and r both small. It then follows straightforwardly that

$$G \sim \frac{2K}{U} \cos \Lambda(x) \quad \text{for } r \text{ small.} \tag{A.6}$$

Although we cannot claim more than plausibility for (A.5), the numerical results from lifting-surface theory do suggest that G tends to zero in proportion to distance from the tip, as (A.6) predicts.

For the delta wing, (A.4) gives $m = s - \frac{1}{2}$, so $0 < m < \frac{1}{2}$, while $n = 0$. hence, by (A.1), the strength and height of the vortex remain finite, while the inboard displacement tends to infinity as the tip is approached.

For the streamwise tip, (A.6) gives $m = n > 0$. (A.1) shows that the lateral displacement is now finite, but the height tends to infinity and the strength tends to zero as the tip is approached. This unrealistic behaviour arises from the rapid variation in σ as $x \to x_t$, which has been ignored in deriving the approximation (25) to the more complete equation (22). A similar difficulty has been discussed in [5], and here we follow the same approach. To obtain a solution to (22) which is more accurate near the streamwise tip, we must suppose that all the terms are of the same order. This is achieved by introducing a stretched streamwise coordinate ξ. The appropriate stretching turns out to be

$$c - X = \alpha^{1/3} \xi, \qquad \sigma = \alpha^{1/6} \tilde{\sigma}_0(\xi), \qquad \tau = \tilde{\tau}_0(\xi). \tag{A.7}$$

Equation (23) then reduces simply to $\tilde{\tau}_0' = 0$. We have just shown that τ_0, as given by (27), takes a finite value, say τ_t, at $x = x_t$, so for this tip solution we can write

$$\tilde{\tau}_0 = \tau_0 = \tau_t. \tag{A.8}$$

We can also write $A(x) = A_t$, and, for a regular tip shape,

$$B_0(x) \sim \lambda^2 (X - c) = -\alpha^{1/3} \lambda^2 \xi,$$

where $\lambda^2 = B_0'(x_t) > 0$, since $\mathrm{d}x/\mathrm{d}X = 1$ at $X = c$. In this way (22) reduces to

$$\tilde{\sigma}_0 \frac{\mathrm{d}\tilde{\sigma}_0}{\mathrm{d}\xi} - \frac{\lambda^2}{\tau_t^2}\xi\tilde{\sigma}_0^2 + \frac{A_t}{8\tau_t} = 0.$$

The solution of this equation which matches the behaviour of σ_0, as obtained from (25), may be written as (see [5] for details)

$$\tilde{\sigma}_0^2 = \pi^{1/2}\frac{A_t}{8\lambda}\mathrm{e}^{\eta^2}\,\mathrm{erfc}\,\eta, \quad \eta = \lambda\xi/\tau_t. \tag{A.9}$$

A composite solution for σ, to leading order, which is uniformly valid up to $X = c$, can be obtained in the usual way [6] by adding the inner and outer solutions and subtracting the outer expansion of the inner solution. We find

$$\frac{\sigma}{\alpha^{1/3}} = \frac{\tilde{\sigma}_0}{\alpha^{1/6}} + \sigma_0 - \left(\frac{A_t\tau_t}{8\lambda^2}\right)^{1/2}(c - X)^{-1/2}. \tag{A.10}$$

It is $\sigma/\alpha^{1/3}$, as given by (A.10), that must be used in place of σ_0 in (28) for z_V, and in (29) for Γ, for wings with streamwise tips. Equation (30) no longer holds for wings with streamwise tips. It is easy to see that the last two terms in (A.10) cancel as $X \to c$, while $\tilde{\sigma}_0$, from (A.9), tends to a finite non-zero limit. Thus we now have finite, non-zero values for the vortex coordinates and strength at the streamwise tip. This improvement is gained at the expense of a less of generality – since the right-hand side of (A.10) is not homogeneous in α, the vortex height and strength no longer scale with powers of α.

Acknowledgments

The suggestion for a treatment of this type came originally from Mr E.C. Maskell. The lifting-surface theory calculations were carried out by Mr S.P. Fiddes.

References

[1] E.C. Polhamus, A concept of the vortex lift of sharp-edged delta wings, based on a leading-edge suction analogy, NASA TN D-3767 (1966).

[2] C.E. Brown and W.H. Michael, On slender delta wings with leading-edge separation, *J. Aeron. Sci.* 21 (1954) 690–694.

[3] J.E. Barsby, Flow past conically-cambered slender delta wings with leading-edge separation, ARC R&M 3748 (1972).

[4] J.E. Barsby, Separated flow past a slender delta wing at low incidence, *Aeron. Quart.* 24 (1973) 120–128.

[5] R.W. Clark, J.H.B. Smith and C.W. Thompson, Some series expansion solutions for slender wings with leading-edge separation, ARC R&M 3785 (1976).

[6] M.D. Van Dyke, *Perturbation methods in fluid mechanics*, Academic Press, New York (1964).

[7] S.P. Fiddes and J.H.B. Smith, Strake-induced separation from the leading edges of wings of moderate sweep, Conference on High angle of attack aerodynamics, AGARD-CP-247 (1979).

[8] R.T. Medan, Aerodynamic loads near cranks, apexes and tips of thin, lifting wings in incompressible flow, Conference on Prediction of aerodynamic loading, AGARD-CP-204 (1977).

[9] R.W. Clark, Non-conical flow past slender wings with leading-edge vortex sheets, ARC R&M 3814 (1976).